Electrochemical Deposition of CoCu/Cu Multilayers: Structural and Magnetic Properties as a Function of Non-magnetic Layer Thickness

Article · March 2018

CITATIONS
0

READS
20

4 authors:

Atakan Tekgül
Uludag University
28 PUBLICATIONS **70** CITATIONS
SEE PROFILE

Hakan Köçkar
Balikesir University
134 PUBLICATIONS **644** CITATIONS
SEE PROFILE

Hilal Kuru
Balikesir University
29 PUBLICATIONS **81** CITATIONS
SEE PROFILE

Mursel Alper
Uludag University
110 PUBLICATIONS **996** CITATIONS
SEE PROFILE

Atakan Tekgül[a,*], Hakan Kockar, Hilal Kuru and Mursel Alper

Electrochemical Deposition of CoCu/Cu Multilayers: Structural and Magnetic Properties as a Function of Non-magnetic Layer Thickness

https://doi.org/10.1515/zna-2017-0332
Received September 18, 2017; accepted December 2, 2017; previously published online January 4, 2018

Abstract: Electrochemical deposition of CoCu/Cu multilayers was performed on titanium substrates from a single bath as a function of the Cu layer thicknesses. The deposition potentials were selected as –1.5 V for the magnetic layers and –0.3 V for the non-magnetic layers with respect to the saturated calomel electrode. The current-time transients were obtained during the deposition process, and the Co layer deposition and capacitive transients were calculated. On the basis of structural analysis, the multilayers were found to be polycrystalline with both Co and Cu layers adopting the face-centered cubic structure. The calculated lattice parameters of the multilayers slightly increase from 0.3585 to 0.3615 nm with increase in the Cu layer thickness, which is consistent with the bulk value of Cu. The interplanar distance of the peaks of the multilayers is closer to that of Cu (d_{111} = 0.2087 nm) and Co (d_{111} = 0.2046 nm), and they become close to that of bulk Cu with increasing Cu layer thickness. In magnetic measurements, the magnetization decreases from 156 to 44 emu/cm^3 depending on the Cu layer thickness. Furthermore, the coercivity of the multilayers increases from 20 to 140 Oe. These values show that the magnetic behaviour of the multilayers lie between those of soft and hard magnetic materials, but the multilayer having 2.5 nm Cu layer thickness shows hard magnetic property. For the CoCu(4 nm)/Cu(0.7 nm) multilayer, the magnetoresistance measurement shows 5.5 % giant magnetoresistance (GMR).

[a]Present address: Akdeniz University, Physics Department, TR-07058, Antalya, Turkey.
***Corresponding author: Atakan Tekgül,** Uludag University, Physics Department, Science and Literature Faculty, TR-16059 Bursa, Turkey, E-mail: atakantekgul@gmail.com.
http://orcid.org/0000-0001-6737-3838
Hakan Kockar and Hilal Kuru: Balikesir University, Physics Department, Science and Literature Faculty, TR-10145 Balikesir, Turkey, E-mail: hkockar@balikesir.edu.tr (H. Kockar), htopcu@balikesir.edu.tr (H. Kuru)
Mursel Alper: Uludag University, Physics Department, Science and Literature Faculty, TR-16059 Bursa, Turkey, E-mail: malper@uludag.edu.tr

Keywords: CoCu/Cu Multilayer; Electrochemical Deposition; Electrochemical Properties; Magnetic Properties; Structural Properties.

1 Introduction

In recent years, much attention has been paid to the production of multilayered systems by electrochemical deposition. Microelectromechanical systems, read heads of hard disk drives, magnetic sensors, and protective coatings are the main potential applications of such systems [1]. Multilayers with different pairs of iron-group metals have been studied, of which the Co/Cu system is an important class for use as magnetic sensors [2–4]. The properties of electrochemically deposited multilayers are dictated by a number of factors including the deposition potential, the electrolyte pH, and the magnetic and non-magnetic layer thicknesses. Among them, the last one is a critical parameter to achieve the structural and functional properties. The non-magnetic layer thickness provides the separation of adjacent magnetic sublayers, and therefore the ferromagnetic and antiferromagnetic behaviour between magnetic layers can be controlled [5]. By using a single bath during the electrochemical deposition process, the noble metal ions are deposited along with the less noble metal ions at higher overpotentials. In this case, the amount of non-magnetic metal in the magnetic layers increases while the thickness of the magnetic layers decreases as a result of the anomalous co-deposition [6]. Consequently, the ferromagnetic sublayers will include non-magnetic materials so that non-magnetic sublayer thickness is higher than the expected value. This results in the change of the interfacial roughness between the layers. Therefore, alignment of ferromagnetic or antiferromagnetic domains between the adjacent magnetic layers changes more sensitively in an external magnetic field.

In the present study, CoCu/Cu multilayers were deposited on Ti substrates from a single bath as a function of the non-magnetic layer thickness, and their electrochemical, structural, and magnetic properties were investigated. In the single bath, the number of Co ions is

typically 55 times more than that of Cu ions. Cu is expected to reduce more easily since it is a nobler metal than Co. However, it is seen that the Co ions inhibit the reduction of Cu ions. The deposition potentials were determined by cyclic voltammograms (CVs), in which –1.5 and –0.3 V versus the saturated calomel electrode (SCE) were used for Co and Cu ions, respectively. In order to examine the effect of the Cu layer thickness on the film properties, the Cu layer thickness was chosen as 0.1, 0.3, 0.5, 0.7, 1.0, 1.3, 1.5, 2.0, and 2.5 nm while the Co layer thickness was kept constant at 4.0 nm. The nominal thickness of the multilayers was 3 μm. Structural analysis of the CoCu/Cu multilayers indicated that they had the face-centered cubic (fcc) structure similar to bulk Cu. However, a splitting of the characteristic peak (220) corresponding Cu(220) and Co(220) was observed in their X-ray diffraction (XRD) patterns. In magnetic measurements, the magnetization was found to be 156 emu/cm^3 at 0.1 nm Cu layer thickness. With increasing Cu layer thickness, this value decreased to 44 emu/cm^3. The coercivity of the multilayers was found to lie between the limits for soft and hard magnetic materials (12.5 Oe $< H_c <$ 125 Oe [7]), assuming the multilayers to have a thickness of 2.5 nm. For multilayers with 0.7 nm Cu layer thickness, the measured magnetoresistance (MR) was 5.5%.

2 Experimental

For the CoCu/Cu multilayer deposition, two-pulse plating from a single bath was applied on Ti substrates. All processes were carried out with a potentiostat/galvanostat having three electrodes, and were controlled by a personal computer. These electrodes were a Ti sheet for the cathode (which was masked with electroplating tape except for an area of 2.9 cm^2 geometrical area), a platinum foil for the anode, and SCE as reference. The Ti sheet had hexagonal close-packed structure and one of its faces was polished mechanically. The pH value of the freshly prepared electrolyte was 2.4 ± 0.1. The concentrations of the solutions were as follows: 0.75 M cobalt sulfate, 0.05 M copper sulfate, 0.25 M boric acid, and 0.01 M sulfamic acid. Cobalt-based multilayers, such as the Ni–Fe system, show anomalous co-deposition [6]. This has to be taken into account during the preparation of the electrolyte, and the solutions prepared have to be cobalt-rich.

For the deposition of the layers, potentiostatic mode was used with SCE. The deposition potentials were determined from the CV of the electrolyte. The ferromagnetic (Co) layers were deposited at a cathode potential of –1.5 V with respect to SCE, and the non-magnetic (Cu) layers were deposited at a potential of –0.3 V versus SCE. The number of bilayers was chosen such that the nominal thickness was about 3 μm. In order to investigate the effect of the non-magnetic layer thickness, the Co layer thickness (t_{Co}) was kept constant at 4 nm and the Cu layer thickness (t_{Cu}) was set to be 0.1, 0.3, 0.5, 0.7, 1.0, 1.3, 1.5, 2.0, and 2.5 nm. For controlling the thickness of the Co and Cu layers, the charge flowing through the system was measured during the potentiostatic pulse. Then, the charge necessary to get the preset nominal layer thickness could be calculated from Faraday's law using (1):

$$d = \frac{Q\eta}{zFA}\frac{M}{\rho} \tag{1}$$

here, Q is the quantity of the deposited metals as a function of deposition time of its metal ion, and z, F, and A are valance electrons of the metal ion, the Faraday constant, and the sample surface area, respectively. In addition, M is the molar weight and ρ is the density of the metal ion. The important parameter in this equation is the current efficiency η, which for the Co-rich layer deposition was calculated by assuming that the deposition took place at 100% current efficiency [5], since hydrogen evolution was negligible.

XRD was used to investigate the structure of CoCu/Cu multilayers using a Philips Analytical XRD system (PW 3040/60 model) with Cu K_α radiation in the scanning range $2\theta = 30°–80°$. In order to obtain quantitative information from the X-ray diffractograms, the FullProf software was used to refine the crystal structure.

The morphology and composition of the multilayers were studied by scanning electron microscopy (SEM) with the energy dispersive X-ray (EDX) attachment (LEO 1530).

The magnetic properties were studied using a vibrating sample magnetometer (VSM, ADE technologies DMS-EV9 Model). MR measurements were carried out in magnetic fields in the range ±1.2 kOe at room temperature with the Van der Pauw (VDP) technique by using (2).

$$\text{MR}\ (\%) = \frac{R(H) - R_{\min}}{R_{\min}} \times 100 \tag{2}$$

In this relation, $R(H)$ is the measured electrical resistance value at any magnetic field, and $R_{\min}$ is the minimum measured resistance. The magnetic field was applied both parallel and perpendicular to the current flowing in the film plane to measure the longitudinal and transverse magnetoresistance, respectively.

3 Results and Discussion

Preliminary information on the optimal potential was obtained from the CV, which is shown in Figure 1. Anodic scan was performed in the range 0 to –1.5 V. In the figure, the Cu ion deposition started at about –0.2 V and then Co with Cu ions began to deposit on the substrate after –0.7 V. Dissolution was observed in the electrolyte at –0.5 V. The dissolution rate increased linearly. Therefore, high and stable deposition potential was chosen at –1.5 V for the Co ions because of the high Co deposition rate. For the Cu ions, –0.3 V deposition potential was determined since Cu ion deposition was expected only between –0.2 and –0.7 V.

In order to obtain information about the deposition processes, the current-time transients were recorded during growth for the first few layers of the multilayers in terms of the Cu layer thickness, which are given in Figure 2a–i. As can be seen from the figure, two anodic

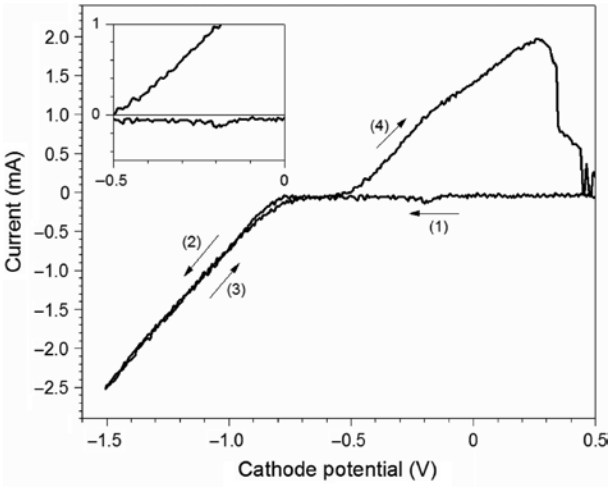

Figure 1: Cyclic voltammetry of the electrolyte containing Co and Cu ions. Arrows indicate the measurement direction.

pulses and a capacitive transition are clearly observed. In the potentiostatic process, two different metal ions are deposited by two pulses from a bath. One of the pulses is the anodic current for the Cu layers, and the other is a high anodic current for the Co layers, as indicated in Figure 2a. Therefore, according to the obtained information from CV, the Co and Cu ions deposit on the substrate at high anodic currents and at low anodic currents, respectively. The capacitive transient occurs after high anodic current since the cathode gains a high potential during this process and this high potential causes the dissolution of the last deposited layer during the switching of the pulse from high to low current. In the figures, the anodic current at the beginning of the deposition process indicates Cu layer deposition with a low current pulse and then the high anodic pulse arises, which points to the Co layer deposition (Cu layer deposition at the same time). After the coverage of the underlying Cu layer with Co, a capacitive transient occurs from a stable negative to a positive current value and the next Cu layer deposition begins in this negative current value. As seen in the figures, the Co sublayers of the multilayer get deposited quickly. This indicates that the number of Cu ions in the electrolyte decreases near the substrate after the deposition of the Cu

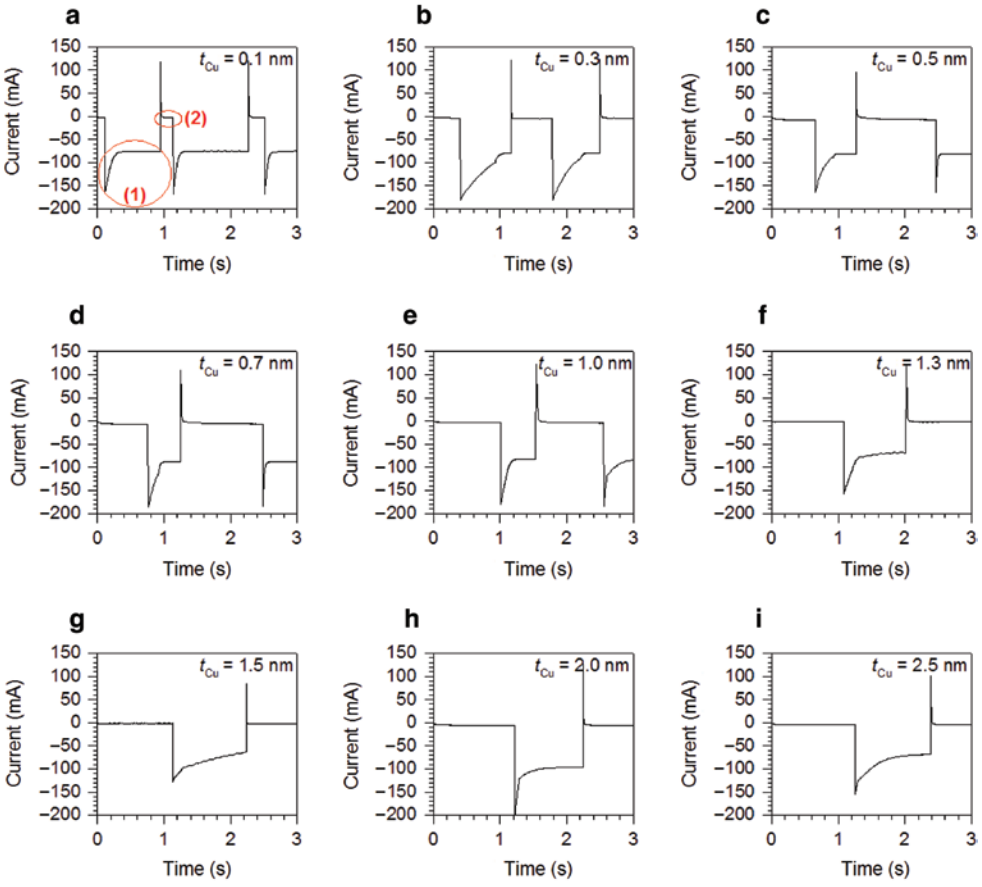

Figure 2: Current-time transients of CoCu/Cu multilayer at (a) 0.1, (b) 0.3, (c) 0.5, (d) 0.7, (e) 1.0, (f) 1.3, (g) 1.5, (h) 2.0 and (i) 2.5 nm Cu layer thicknesses. (1) and (2) indicate Co and Cu layer deposition, respectively.

sublayer; moreover, the Co ions could be easily deposited in the magnetic sublayers. In addition, Cu is expected to reduce more easily since it is nobler than Co. However, the anomalous co-deposition [6] occurs during the deposition so that the Co ions inhibit the reduction of Cu ions and thus the Cu concentration is lower than that of Co in the electrolyte. Moreover, Co ions at high concentration prevent the deposition of Cu ions, and hence fewer noble metal ions preferentially deposit on the substrate. In summary, against a decrease in the magnetic material due to Co dissolution, anomalous co-deposition supports the needed amount of Co in the magnetic layers.

From the current-time curves, the current densities of the multilayers were calculated. The results are given in Figure 3. As seen in the figure, the Co and Cu layers deposit at ~60 mA/cm^2 (black circle) and 40 mA/cm^2 (triangle), respectively. The results show that the layers grow at almost the same the current densities. The capacitive transient is quite low, which means that the dissolution of the Co layer occurs in small amounts. Using these curves, the nominal magnetic and non-magnetic layer thicknesses (d) were calculated based on Faraday's law using (1). The nominal and expected layer thicknesses are plotted in Figure 4. Here, a linear fit was employed, and the obtained slope was found to be 1.007. This indicates that the calculated thicknesses are closer to the expected thicknesses.

Figure 5 shows the refined XRD patterns of the multilayers. All data are normalized in the figure. In the figure, the grey circles are the observed intensities, I_{obs}, and the black thick lines are the calculated intensities, I_{calc}. $I_{obs} - I_{calc}$ is the difference spectrum (black line). The

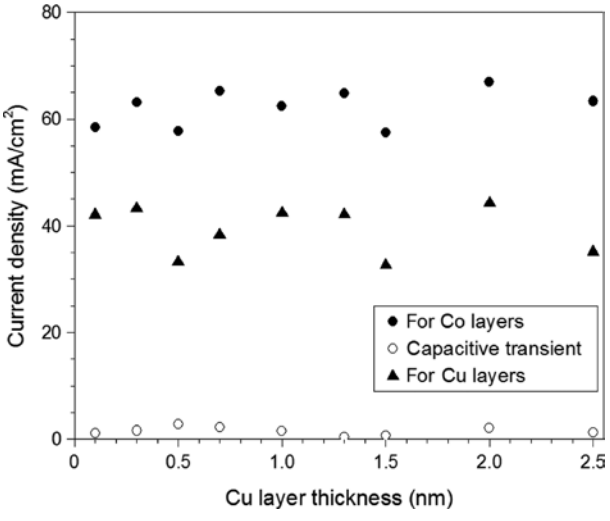

Figure 3: Current density versus Cu layer thickness of the all multilayers for both Co and Cu layers and capacitive transients.

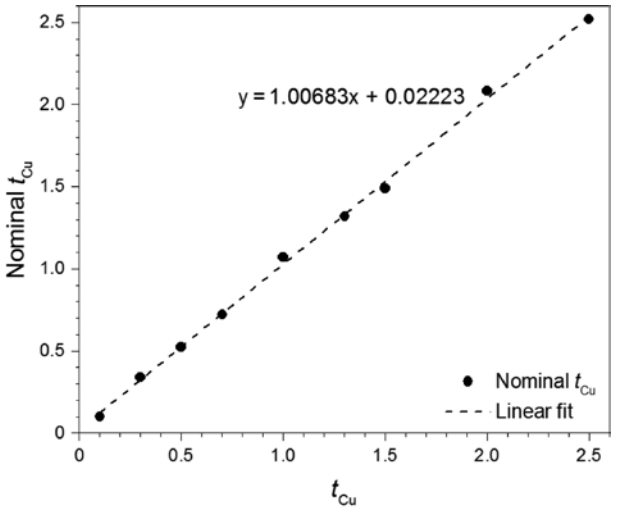

Figure 4: Calculated nominal Cu layer thickness of the multilayers from Faraday's law.

Bragg positions are shown in the lower part of each figure. Co and Cu structures are indicated on the right side of the patterns. The peaks appearing at $2\theta \approx 43°$ and 50° are related to the (1 1 1) and (2 0 0) planes. Also, the two peaks at 72° and 74° belong to the (2 2 0) planes of Cu and Co, respectively. These results show that all multilayers are polycrystalline with both magnetic and non-magnetic layers adopting the fcc structure. However, the intensity and position of the peaks at 72° and 74° change with the Cu layer thickness and, as seen in the figure, the intensity of the Co(2 2 0) peak is higher than that of the Cu(2 2 0) peak at 0.1 nm Cu layer thickness. With increasing Cu layer thickness, the Cu(2 2 0) and Co(2 2 0) peaks are similar and their intensities are almost the same until 0.7 nm Cu layer thickness. After this Cu thickness, the Cu(2 2 0) peak is higher than that of Co(2 2 0). A remarkable point is that the Co(2 2 0) and Cu(2 2 0) peaks come close to each other and begin to merge at 2.5 nm Cu layer thickness. This means that the crystal structure of the multilayers completely adopts the fcc structure of bulk Cu at 2.5 nm Cu layer thickness.

Using the FullProf software, the lattice parameters and the inter-planar distance of the two strongest peaks were calculated. The obtained values are presented in Figure 6a and b. the lattice parameter of the multilayers increases with the Cu layer thickness and these values begin to come close to that of bulk Cu (0.3615 nm). The inter-planar distances of the multilayer change between 0.2050 and 0.2100 nm for d_{111} and between 0.1790 and 0.1850 for d_{200}. They have similar values with increasing Cu layer thickness, and also these values are closer to the inter-planar distance of Cu ($d_{111} = 0.2087$ nm [8]).

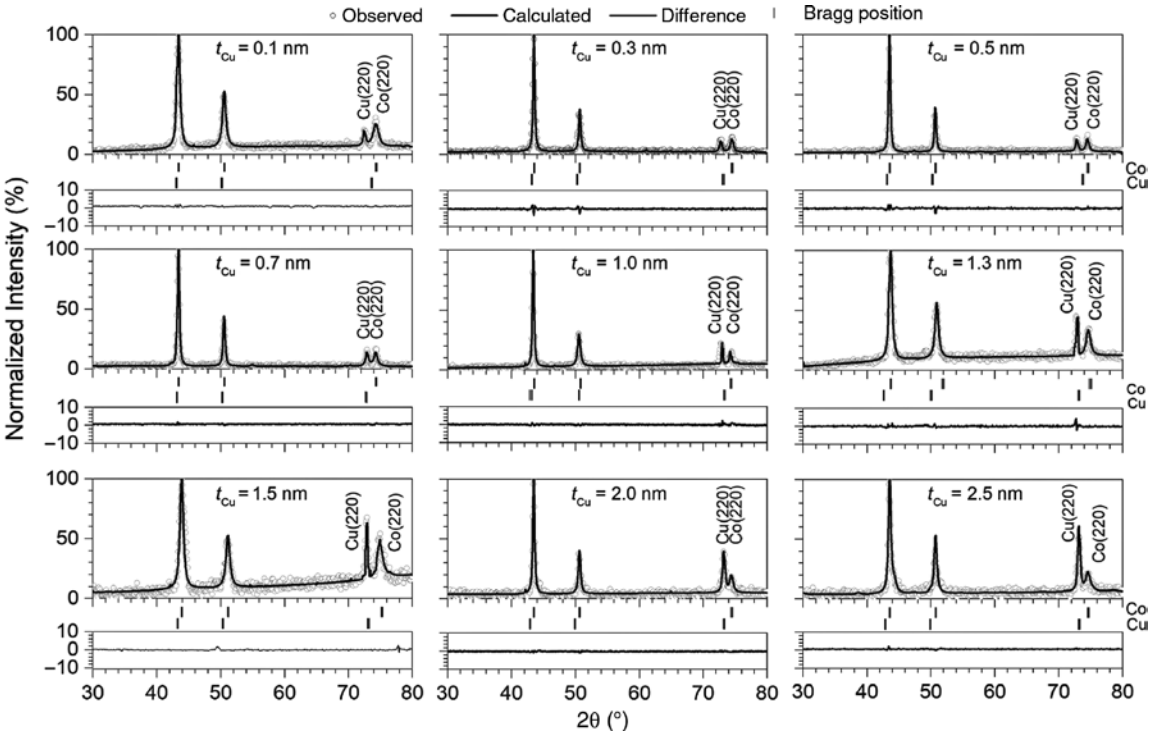

Figure 5: Refined XRD patterns of the multilayers in the range 30°–80°. Grey circle is the observed pattern, black thick line is the calculated pattern, and the difference of these is shown as black line patterns at bottom in each figure. Bragg positions of all structures are indicated.

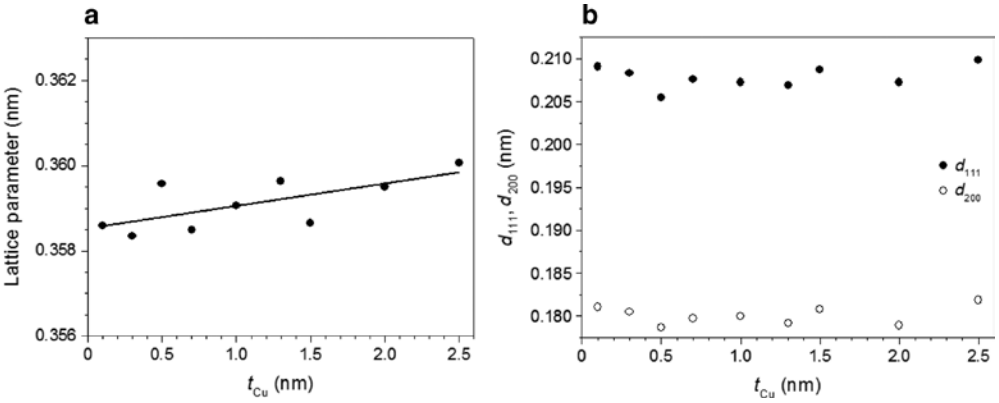

Figure 6: (a) Lattice parameters and (b) inter-planar distances of the multilayers as a function of Cu layer thickness.

These results indicate that the multilayers show the properties of bulk Cu structure with increasing Cu layer thickness.

The preferred orientations of the multilayers were studied using the texture coefficient given by the equation in [9]. The calculated values are given in Table 1. The results show that the multilayers having Cu layer thickness of 0.1, 0.5, 1.3, and 2.5 nm prefer to grow in the [2 2 0] direction predominantly. According to these findings, most of the multilayers have the same texture. And the other multilayers show random orientation. This suggests that the crystal orientation of some of the multilayers changes depending on the Cu layer thickness.

The morphological and compositional analyses were performed by SEM with EDX. The SEM images of all multilayers were taken at 5.9 mm working distance by applying 15 kV accelerating voltage. Figure 7 presents the SEM image of the CoCu(4 nm)/Cu(1 nm) multilayer. As seen in the figure, the surface morphologies of the multilayers are similar and show a uniformly grained surface. The composition of the multilayers is given in Table 1. EDX analysis reveals that the composition is close to that of the

Table 1: Preferred orientations and EDX results of the multilayers.

t_{Cu} (nm)	M_{111}	M_{200}	M_{220} for Cu	M_{220} for Co	Compositional analysis (wt%) Co/Cu
0.1	0.6446	0.6108	1.7561	0.9885	97.10/2.90
0.3	0.9904	0.7003	1.2426	1.0666	92.71/7.29
0.5	0.4478	0.5276	1.5897	1.4348	87.13/12.87
0.7	1.0554	0.8142	0.9029	1.2276	83.24/16.76
1.0	1.0694	0.8495	0.8976	1.1835	78.32/21.68
1.3	0.7443	0.8418	0.9183	1.4956	74.18/25.82
1.5	0.9570	0.9007	0.9586	1.1837	72.72/27.28
2.0	0.5987	0.7048	1.4138	1.2828	65.35/34.65
2.5	0.7446	0.6659	1.5884	1.0011	61.30/38.70

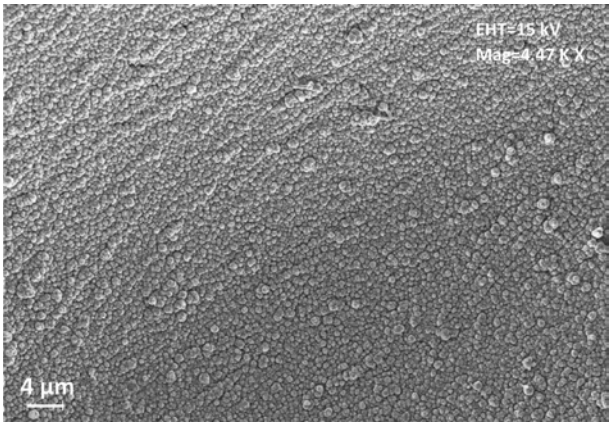

Figure 7: SEM image of the CoCu(4 nm)/Cu(1 nm) multilayer.

expected thickness of the multilayers and the Cu amount is about 1 % in the Co layer.

Figure 8 shows the hysteresis loops of the multilayers measured at 2 kOe external magnetic field. The obtained magnetization indicates that the hysteresis loops of the multilayers did not reach saturation in this field. This non-saturation state in hysteresis is due to the presence of a fraction of super-paramagnetic region in the magnetic layers. Therefore, the magnetic field strength is not enough to change the direction of the magnetic moments. The magnetization of the multilayers decreases from 156 to 44 emu/cm^3 with increasing Cu layer thickness under 2 kOe external magnetic field. The obtained magnetization and the coercivity values are presented in Figure 9. Until 1.5 nm Cu layer thickness, a sharp decrease in the magnetization was observed, and then similar values were found. A lower magnetization implies antiferromagnetic coupling between the magnetic layers. The coercivity (H_c) of multilayers increases from 20 to 140 Oe as a result of the Cu layer thickness. These results show that the H_c values are in between the limits of soft and hard magnetic properties (12.5 Oe < H_c < 125 Oe) [7], which is expected for a multilayer having 2.5 nm Cu layer thickness.

For the multilayer with 0.7 nm Cu layer thickness, the magnetoresistance measurement was performed at room temperature using the VDP method with the current flowing in the film plane. As seen in Figure 10, both

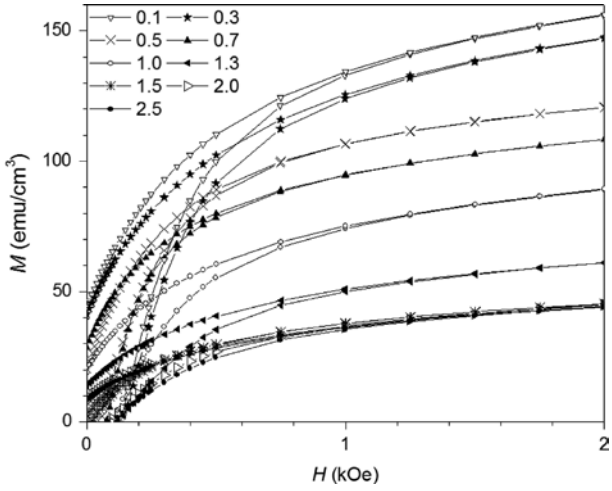

Figure 8: *M*–*H* curves of the CoCu/Cu multilayers in the range of 0–2 kOe.

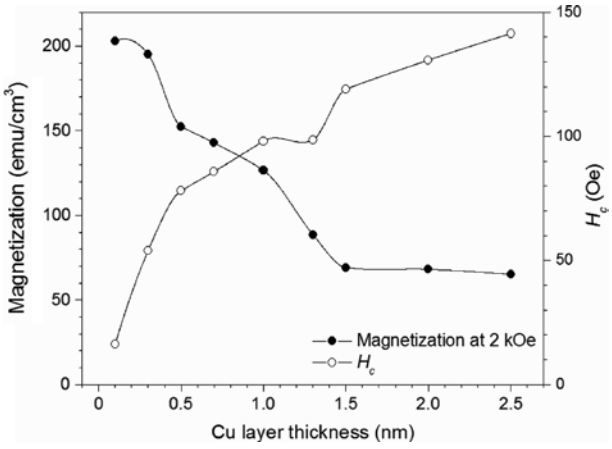

Figure 9: Evolution of the magnetization at 2 kOe and H_c of the multilayers due to the Cu layer thickness.

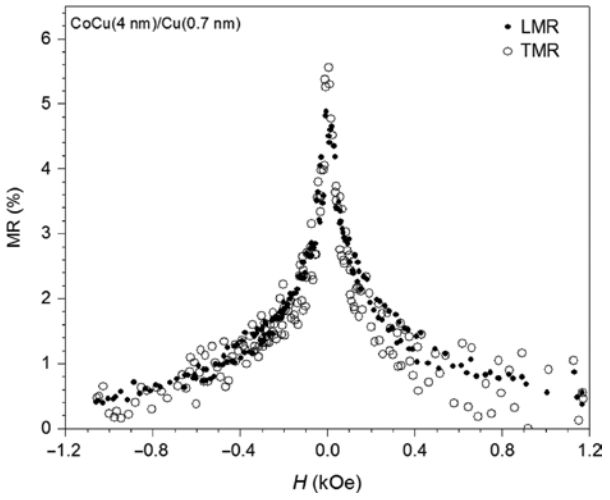

Figure 10: MR curves of the CoCu(4 nm)/Cu(0.7 nm) multilayer under 1.2 kOe magnetic field. Black and hallow circles show the LMR and TMR curves.

longitudinal and transverse magnetoresistance decrease as the magnetic field increases, that is, the multilayer has the giant magnetoresistance (GMR) effect, which is due to its multilayer structure. As explained in [10], the critical thickness of ferromagnetic or antiferromagnetic coupling of the adjacent magnetic layer is 1 nm for the non-magnetic layer, and in this sample the increase of the 0.7 nm Cu layer thickness occurs as a result of the dissolution. Therefore, the thickness of the Cu layer is close to the critical thickness (1 nm). Consequently, antiferromagnetic coupling is dominant and high GMR (5.5%) is observed at room temperature.

4 Conclusion

The effect of non-magnetic layer thickness on the magnetic CoCu/Cu multilayers was investigated by varying the Cu layer thickness. The multilayers were grown on Ti substrates under potentiostatic control at room temperature. From the structural results, the multilayers have characteristic (1 1 1), (2 0 0), and (2 2 0) peaks of the fcc lattice. The calculated lattice parameters and inter-planar distances showed that the multilayers behave like bulk Cu due to the Cu layer thickness. Consequently, the magnetizations gradually decreased with the increase of the Cu layer thickness. An increase was observed with increase of the Cu layer thickness in the coercivity of the multilayers, and these values of multilayers are between the soft and hard magnetic limits, which is excepted for a multilayer having 2.5 nm Cu layer thickness. For the CoCu(4 nm)/Cu(0.7 nm) multilayer, the measured GMR value is 5.5 %. Therefore, it is feasible to produce multilayer with the desired properties depending on the Cu layer thickness for potential applications in magnetic sensor technology.

Acknowledgements: The authors wish to thank Dr. H. Guler, Balikesir University, Balikesir, Turkey, for XRD measurements. This work was partly supported by Uludag University under Funder Id: 10.13039/501100004401, Grant no. UAP(F)-2010/56. The authors would also like to thank the State Planning Organization, Turkey, for the VSM system provided under Funder Id: 10.13039/501100007628, Grant no. 2005K120170.

References

[1] N. Smith, A. M. Zeltser, and M. R. Parker, IEEE Trans. Magn. **32**, 135 (1996).
[2] I. Bakonyi, L. Peter, Z. E. Horvath, J. Padar, L. Pogany, et al., J. Electrochem. Soc. **155**, D688 (2008).
[3] M. Safak, M. Alper, and H. Kockar, J Nanosci. Nanotechnol. **8**, 854 (2008).
[4] M. Haciismailoglu, M. Alper, and H. Kockar, Sens. Lett. **11**, 106 (2013).
[5] I. Bakonyi and L. Peter, Prog. Mater. Sci. **55**, 107 (2010).
[6] H. Kuru, H. Kockar, M. Alper, and O. Karaagac, J. Magn. Magn. Mater. **377**, 59 (2015).
[7] D. Jiles, Introduction to Magnetism and Magnetic Materials, Chapmanand Hall, London 1991.
[8] A. Taylor and R. W. Floyd, Acta Crystallogr. **3**, 285 (1950).
[9] B. D. Cullity, Elements of X-ray Diffraction, Addison-Wesley, Massachusets 1978, p. 547.
[10] I. Bakonyi, E. Simon, B. G. Toth, L. Peter, and L. F. Kiss, Phys. Rev. B **79**, 174421 (2009).